# INITIAL FLIGHT TESTS OF AN AUTOMATIC SLUNG LOAD CONTROL SYSTEM FOR THE ACT/FHS

Hyun-Min Kim, Daniel Nonnenmacher, Joachim Götz
German Aerospace Center (DLR), Institute of Flight Systems
Lilienthalplatz 7, 38108 Braunschweig, Germany

Pascal Weber, Edgar von Hinüber, Stefan Knedlik
iMAR Navigation GmbH
Im Reihersbruch 3, 66386 St. Ingbert, Germany

### ABSTRACT

An automatic slung load control system for the research helicopter ACT/FHS (Active Control Technology / Flying Helicopter Simulator) of the German Aerospace Center (DLR) has been developed and initially tested in flight. The external load is suspended from a rescue hoist which was mounted at the ACT/FHS for flight test purposes. For the load motion detection an optical-inertial sensor system was developed. The sensor system provides estimations of the cable length and cable angle as well as cable angle rates for the slung load control system. Flight testing of the sensor system proved that the optical marker is detected consistently and accurately for cable length up to 50 m. Furthermore, the estimated load motion signals can be used for the control system. To demonstrate the overall system's functionality, an initial control system for damping of the pendulum load motion was designed and flight tested. The automatic function of the control system was effective in damping the load pendulum motion for a fixed cable length. Under piloted control the slung load damping system showed deficiencies. When actively controlling the helicopter, the pilot acted against the control system resulting in an adverse effect in load damping. Overall, for the first time, a slung load control system for a load suspended from a rescue hoist could be demonstrated successfully.

### Abbreviations

| | |
|---|---|
| ACT/FHS | Active Control Technology / Flying Helicopter Simulator |
| ADS-33 | Aeronautical Design Standard 33 |
| AFDD | US Army Aeroflightdynamics Directorate |
| ALDS | Automatic Load Damping System |
| Blob | Binary Large Object |
| BMWi | *Bundesministerium für Wirtschaft und Energie* (German Federal Ministry of Economics and Energy) |
| BURRO | Broad Area Unmanned Responsive Resupply Operations |
| CAN | Controller Area Network |
| DLR | *Deutsches Zentrum für Luft- und Raumfahrt e.V.* (German Aerospace Center) |
| DOF | Degrees of Freedom |
| DSP | Digital Signal Processor |
| EKF | Extended Kalman Filter |
| FOV | Field of View |
| GNSS | Global Navigation Satellite System |
| HALAS | *Hubschrauber-Außenlast-Assistenzsystem* (Helicopter Slung Load Assistence System) |
| HQ | Handling Qualities |
| IMU | Inertial Measurement Unit |
| LMR | Load-Mass Ratio |
| MEMS | Micro Electro Mechanical System |
| MTE | Mission Task Element |
| RASCAL | Rotorcraft Aircraft System Concepts Airborne Laboratory |
| RLC | Run Length Code |
| RS232, RS422 | Technical standard for data interfaces |
| SCAS | Stability Control Augmentation System |
| iVRU | iMAR Vertical Reference Unit |

### Symbols

| | |
|---|---|
| $A_{GM}$ | Gain margin (dB) |
| $G_{AM}$ | Transfer function gain modulation |
| $G_{PM}$ | Transfer function phase modulation |

| | |
|---|---|
| $G_R$ | Transfer function controller |
| $G_s$ | Transfer function plant |
| $G_{\delta_x \dot{\vartheta}_C}$ | Transfer function of control input to cable angle rate in longitudinal axis |
| $G_{\delta_y \dot{\varphi}_C}$ | Transfer function of control input to cable angle rate in lateral axis |
| $J$ | Performance index |
| $K_V$ | Static amplification factor |
| $L$ | Cable length (m) |
| $g$ | Gravity constant (m/s$^2$) |
| $k_{0dB}$ | Proportional Gain |
| $m_{PM}$ | Amplitude response correction factor |
| $m$ | Mass (kg) |
| $s$ | Laplace variable |
| $\Phi_{PM}$ | Phase margin (deg) |
| $\delta_x$, $\delta_y$ | Longitudinal, lateral control input (%) |
| $\phi$, $\theta$ | Roll, pitch attitude (deg) |
| $\varphi$, $\vartheta$ | Lateral, Longitudinal cable angle |
| $\omega_{E1}$, $\omega_{E2}$ | Cut-off frequencies phase modulation (rad/s) |
| $\omega_{E3}$, $\omega_{E4}$ | Cut-off frequencies gain modulation (rad/s) |
| $\omega_P$ | Pendulum frequency (rad/s) |
| $\omega_d$ | Gain crossover frequency (rad/s) |

**Indices**

| | |
|---|---|
| SCAS | Stability Control Augmentation System |
| ALDS | Automatic Load Damping System |
| Act | Actuator |
| C | Cable |
| L | Load |
| H | Helicopter |
| e | Earth-fixed system |
| cmd | Command |
| perc. | Percental |

## 1. INTRODUCTION

With the ability to hover and to operate at low speed, helicopters are widely used to transport external loads as a slung load. Transporting bulky cargo to or from remote locations, firefighting, construction work, disaster relief and rescue missions are typical slung load operations. The load is suspended at the helicopter with one or more slings representing a pendulum. Manoeuvring the helicopter and external disturbances excite the load motion resulting in a lightly damped load pendulum motion. Flying with a slung load is a demanding task for the flight crew since the pilot has to control the helicopter and avoid excessive load swinging. Generally, the pilot has no direct view on the load and has to rely on verbal instructions of crew members or on auxiliary devices such as a mirror. In the field of aerial work where single-piloted operations are common, the pilot has to control the helicopter with the slung load and monitor the system at the same time. This leads to high workload, particularly when multiple flight cycles have to be flown [1].

A systematic study of how an external load affects the pilot's ability to perform manoeuvres and impacts the Handling Qualities (HQ) of the helicopter is presented in Ref. [2, 3]. There are no current quantitative requirements for external load operations in the Aeronautical Design Standard for rotorcraft (ADS-33-PRF [4]). Initial efforts to develop new criteria have been performed by conducting flight test series of a UH-60 helicopter with an external load [3]. A database of quantitative and qualitative data represented by frequency response data and HQ ratings with pilot comments respectively was generated. Based on this, new criteria for predicting HQ rating for external load operations were proposed. As a result of the study it was stated that the combination of heavy loads and long sling lengths had the most significant impact on aircraft handling, as the load motion induces an unpredictable aircraft response. It was concluded that the newly proposed criteria correlate well with pilot comments and HQ ratings from flight test.

### 1.1. Literature overview

Up to now, numerous concepts and systems for increasing the damping of the external load modes and precision load positioning have been proposed and flight tested. A comprehensive overview of the variety of external slung load control systems is given in Ref. [5, 6] classifying the concepts into direct on-load and indirect load control. These concepts address the load control by exertion of forces and moments directly on the load and by movement of the helicopter respectively. Due to the lower system complexity and weight the indirect load control method has a higher potential of utilisation as last research programs and military applications prove. The relevant systems which are known to have been tested in flight are discussed below.

As an unmanned full-size helicopter, the system BURRO is an autonomous external cargo delivery system that uses a mechanical load measurement (i.e. the lateral trolley position and longitudinal hook position are used for rotor feedback [7, 8]). In the field of piloted operations, Ivler et al. [5] designed a control system for the RASCAL JUH-60 helicopter not only addressing load damping characteristics but also acceptable HQ. The control system used inertial load motion measurements and was designed with the focus of HQ based on the external load HQ criteria proposed in Ref. [2]. In this work, the benefit of the control system in piloted slung load operations has been demonstrated through flight tests.

Several works relating to the external load control by helicopter motion have been demonstrated for small-size helicopters. Bisgaard et al.[9] developed a control system for the AAU Bergen Industrial Twin using an optical measurement consisting of a camera and a visual marker on the load for measuring the pendulum motion. A pin was attached to the marker so that the orientation of the load could be measured additionally. The same optical system was also used for the small-size helicopter GTMax [10, 11]. Both systems were capable of performing a load trajectory following. Bernard et al. [12] developed a multi-lift transportation system with three model helicopters. The orientation of the cables relative to the helicopters was measured mechanically at the suspension point. In addition, the cable force was measured with a force sensor for increased robustness of the control system.

### 1.2. DLR activities

DLR's (*Deutsches Zentrum für Luft- und Raumfahrt*, German Aerospace Center) research activities regarding external load control were initiated with an indirect load control system based on the principle of a flight director [13, 14]. In cooperation with iMAR Navigation GmbH, a display system for the pilot using load measurement was developed and flight tested with two different helicopter types. For the Bo-105 tests, the load measurement was provided by an inertial system whereas for the CH-53G tests an optical system was used. The display system was demonstrated to be effective in damping the load motion for both helicopter types. In the next step, the manual system was developed to the automatic approach within the project HALAS (*Hubschrauber-Außenlast-Assistenzsystem*, Helicopter Slung Load Assistence System). Funded by the BMWi (*Bundesministerium für Wirtschaft und Energie*, German Federal Ministry of Economics and Energy), the project's objectives were the development and demonstration of an automatic slung load control system for DLR's fly-by-wire/-light research helicopter ACT/FHS [15]. The project was carried out by DLR and iMAR Navigation GmbH. The ACT/FHS was equipped with a rescue hoist and an optical-inertial sensor for load measurement. The use of an external hoist as load suspension system allows covering winch operations as a special case of slung load operations and taking into account of variable cable lengths, but leading to some challenges in flight tests. One of the challenges was the limited allowable cable angle in lateral direction to prevent unfavourable contact of the cable with the landing gear. In order to demonstrate the general functionality of the overall system, a first controller for damping the pendulum load motion was developed. Based on previous theoretical works at DLR [16], a controller using cable rate feedback was designed. The initial flight tests of the overall system took place in 2013 (see Fig. 1).

### 1.3. Paper objectives

This paper presents results of the initial flight tests of an automatic slung load control system for the ACT/FHS with a rescue hoist. More specifically, the features of the sensor will be described in detail and flight data of the load motion measurement will be shown. A first control system for slung load damping using the sensor data was developed. The structure of the slung load damping controller will be

Figure 1: Flight test of DLR's research helicopter ACT/FHS with an external load

presented and the optimisation process will be described. Finally, the data of the overall system in closed-loop configuration will be given and the findings discussed. The paper closes with an outlook how the system will be used for future research works.

## 2. Slung load control system for the ACT/FHS

### 2.1. Problem description

The function of the automatic slung load control system can be divided into the two areas load stabilisation and load positioning. The load stabilisation function addresses the forward flight case when the pilot has to control both the helicopter and the slung load at higher flight speed and an increase in the damping of the load pendulum motion is desired to augment the flight safety. A pilot assistance function for load positioning is provided at low speed and hover when precise load handling is required (e.g. load pick-up or set-down).
The ACT/FHS is equipped with a side-mounted rescue hoist. One of the reasons for choosing the rescue hoist as suspension system for the external load was the ability to vary the sling length up to 50 m. It is well known that the sling length determines the frequency of the load modes and has a main influence on the stability of these modes as was shown in the parametric stability analysis in Ref. [6]. The rescue hoist enables the testing of arbitrary sling lengths during one flight, so that control system designs can be evaluated easily for different sling load configurations. The consideration of rescue hoist operation as a special case of slung load operation is possible and represents a realistic application with the ACT/FHS, a modified EC135 helicopter which is a light multi-purpose helicopter and often used for rescue hoist operations.
The main drawback of the rescue hoist position is the large lateral offset of the suspension point resulting in a coupling between the helicopter's motion in the yaw axis and the load

motion. In addition, due to safety issues the allowable lateral pendulum angle is more restricted than for central load suspension since a contact of the cable with the landing gear should be avoided. For this reason, during the initial flight tests the sensor and control system were tested mainly in the longitudinal axis. The collection of quantitative flight data (e.g. frequency response data) was not possible because of the safety issues and the limited testing time. After gaining experience with external slung load handling, it is intended to produce frequency sweep data in the future for model validation and control system verification.
Another shortcoming is the low allowable load mass for the rescue hoist (i.e. 230 kg). The high weight of ACT/FHS's experimental system restricted the load mass further to 100 kg. The impact of the external load on the helicopter motion can be estimated with the load-mass-ratio (LMR) parameter. This is the ratio between the load mass and the overall helicopter mass. With the tested external load, for the ACT/FHS the LMR is 0.04. Referring to the results of the study in Ref. [3] which states that the influence of the load was noticeable to the pilots for LMR of 0.12, it was assumed that the load has no significant impact on the motion of the ACT/FHS, at least in the perception of the pilots. This was confirmed by the pilots in the flight tests. Following this, no studies for investigating the HQ degradation due to a suspended load were planned for the work presented in this paper.

### 2.2. Functionalities of the sensor system

Fig. 2 shows the hardware components of the system, the rescue hoist and the optical-inertial sensor system developed by iMAR Navigation GmbH. The optical-inertial sensor system consists of an optical-inertial sensor and an optical marker. The optical-inertial sensor is mounted under the boom of the rescue hoist. A smart camera, a Micro Electro Mechanical System (MEMS) based GPS-aided vertical reference unit (iVRU) and a control unit are integrated in the compact and robust sensor housing. The optical-inertial sensor looks downwards and tracks the position of the optical marker by a sophisticated image data processing algorithm. An estimator calculates the cable angle and cable angle rates based on the detected marker position and inertial measurements. In addition, the actual suspension length can be estimated by the sensor's control unit. The optical marker is fixed over the bumper of the cargo hook on the cable and is used to mark the load position. In Fig. 3 the optical marker without the cover is depicted. A more detailed system description of the ACT/FHS with its hardware components for the slung load control was presented in Ref. [6].


Figure 2: ACT/FHS with rescue hoist and slung load sensor system

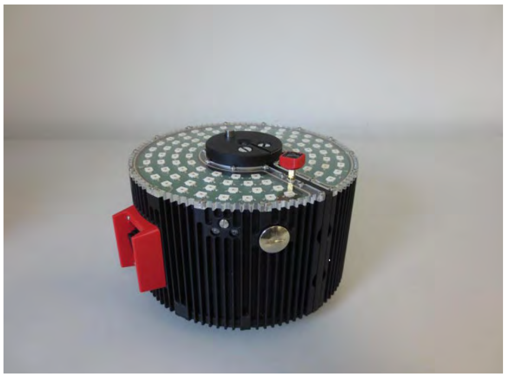

Figure 3: Optical marker without cover

#### 2.2.1. Image processing

To detect the light signal of the optical marker in the camera image, appropriate algorithms have been developed and implemented on the digital signal processor (DSP) of the smart camera. After an image has been acquired by the smart camera, the grey scale image is binarised by means of threshold filtering in preparation for blob (Binary Large Object) analysis. In low visibility conditions (e.g. due to fog, rain, snow, smoke and dust), the binarisation threshold can be adjusted by the software. Then the binary image is converted into run length code (RLC) and the RLC is labelled to identify regions of connected white pixels. To determine the position of the optical marker in the camera image, the centre of the area and the size of each white blob are determined.
The marker signal detected by the camera is dilated five times by image processing methods, so that the marker appears as one single blob in the processed camera image over the entire measuring range from 3 m to 50 m. The size of the marker in the camera raw image can be deter-

mined by the intercept theorem if the cable length and the focal length are known. The cable length is predicted by the Kalman filter. To calculate an estimation of the expected marker blob size, the size of the marker in the camera raw image as well as the calibration data of the optical sensor are used. The difference between measured and estimated marker blob size as well as the position of the optical marker in the camera image, which is predicted by the Kalman filter, are used to separate the real marker blob from any other possible interference blobs.

#### 2.2.2. Video data recording

Video data of the smart camera are transferred to the experimental system of the ACT/FHS and recorded. After a flight test, the video data can be replayed and used to verify and validate the image data processing algorithm. The smart camera transfers either unprocessed image data or processed image data, depending on a camera setting. This camera setting can be changed at any time during the flight test.

#### 2.2.3. Inertial measurement unit

The optical-inertial sensor contains a vertical reference unit from iMAR Navigation GmbH. It features three advanced MEMS gyros (< 0.01 deg/s short time bias stability) and three advanced MEMS accelerometers (< 5 mg), an L1 GNSS (Global Navigation Satellite System) receiver and an integrated powerful microprocessor. Interfaces are CAN (Controller Area Network), RS232 or RS422.
iMAR's advanced so called 'No Aiding for Attitude Algorithm' (NoA$^2$ algorithm) is implemented, which has been initially developed for applications where no redundant aiding information from an external source (such as a GNSS) is available, and provides good attitude performance both under static and dynamic conditions. This algorithm is based on an Extended Kalman Filter (EKF), which internally uses very general motion constraints. iMAR's vertical reference unit (iVRU-BB) provides the helicopter's accelerations and angular rates as well as the helicopter's attitude. Attitude accuracy is less than 1 deg with velocity aiding.
The control unit processes either the data provided by the iVRU-BB contained in the optical-inertial sensor system or the data provided by the reference system of the helicopter, depending on a control unit setting. This control unit setting can be changed at any time during the flight test.
Inertial measurements and attitude obtained from both systems, iVRU in the optical-inertial sensor and reference system of the helicopter, are recorded during the flight tests and are compared for performance evaluation.

#### 2.2.4. Load motion estimation

The position of the optical marker measured by the smart camera and the helicopter's attitude provided by the iVRU are observations for the Kalman filter implemented on the control unit in the optical-inertial sensor system.
The 3-dimensional model is based on equations of motion for a point mass pendulum with unknown length and with a suspension point somewhere in the coordinate frame of the camera. The vector to be estimated comprises of 7 components; cable angles around two axes, offsets of these cable angles, appropriate rates, and length of the pendulum. The system provides both inertial and relative load motion information. For the case that the optical marker is outside the camera's field of view (FOV) or the optical marker cannot be detected with sufficient accuracy for a short time, the predicted estimates of the Kalman filter are used.

#### 2.2.5. Synchronization of image acquisition and light emitting

The optical marker can be operated in two modes: continuous mode and trigger mode. In continuous mode, the optical marker emits light continuously. In trigger mode, the image acquisition of the smart camera and the light emitting of the optical marker are synchronized and the optical marker emits light only during the shutter time of the smart camera. This results in reduced power consumption of the optical marker. By reducing the power consumption of the optical marker, the operation time can be extended or a more compact accumulator can be used as power supply and the weight of the optical marker can be reduced.

#### 2.2.6. Experimental display for slung load control

To support the experimental pilot during the flight tests, a graphical display was developed, showing the actual load position by means of inertial pendulum angles and giving status information of the slung load sensor and control system (see Fig. 4). The center point of the rings represents the suspension point at the rescue hoist. Usually, in rescue hoist operation the pilot has no indication of the load position and therefore has to rely on the verbal instructions of the hoist operator. During the first flight the pilots appreciated the display as a very helpful instrument as the communication with the hoist operator could be minimised.

### 2.3. Control system design

In a first approach the control system for damping the load pendulum motion was designed by the extension of the helicopter's SCAS system. The extension was realized by a feedback loop of the load motion measurement after the proposed control law of Ref. [16], which uses lead and lag

Figure 4: Slung load display showing the inertial cable angles

filter elements in the feedback paths. The parameters of the filter elements were optimised by an automated loop-shaping algorithm to achieve good load damping characteristics.

### 2.3.1. Model for control design

A linear six degrees of freedom (DOF) helicopter model, identified using flight test data of the unloaded ACT/FHS, was used for the control law design. This model is extended by nonlinear terms of the differential equations. Additionally it is coupled with a nonlinear slung load model. The cable is modelled as a simple massless spring-damper system and the load as a point mass with drag-only force in direction of the airflow [6]. Structural notch filters, limiters of actuator position commands as well as the actuator dynamics are included in the model used for control law design and optimisation.

As a part of following works, the 6DOF bare airframe model will be replaced by a higher order model - named as 11DOF model - which incorporates the coupled rotor-body dynamics in form of the coupling of regressive rotor flap and lag motion with the body motion. The frequency responses in the pitch axis of both 6DOF and 11DOF model in Fig. 5 show that the high order model describes the helicopter response ('flight data') more accurately. Clearly, in the high frequency range the 6DOF model does not catch up with the helicopter response. The ACT/FHS with its bearingless main rotor exhibits a coupled regressive lead-lag and body motion mode, known as air resonance mode at 12 rad/s. This mode is modelled as a complex zero-pole pair (dipole) and also not present in the 6DOF model. The coherence in Fig. 5 gives a good measure of the quality of the frequency response and a value above 0.6 is considered acceptable. The high coherence in the high frequency range and the good match of the model's response indicates that the 11DOF model simulates the helicopter response adequately.

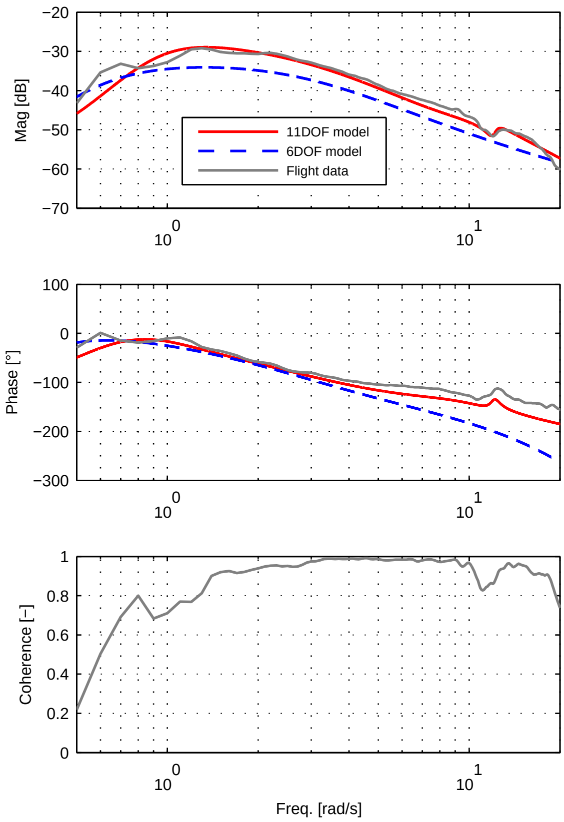


Figure 5: Pitch rate response from longitudinal input in hover: 6DOF and 11DOF model compared to flight data of the unloaded ACT/FHS

### 2.3.2. Controller Structure

The automatic load damping system (ALDS) is designed to extend the functionalities of the helicopter's stability and control augmentation system (SCAS) (see Fig. 6). The SCAS is fed with information delivered by the ACT/FHS sensors (e.g. the air data system and the inertial navigation system). To improve the dynamic stability, the angular rates of the helicopter are fed back in the SCAS using proportional and integral control structures in each axis. The proportional and integral gains are adjusted to realise an attitude command in pitch and roll axis as well as a rate command in yaw and vertical axis. In the vertical axis, the pilot is supported additionally by a height hold function. The SCAS also includes a filter to suppress the air resonance mode [17].
The optical-inertial slung load sensor delivers the longitudinal and lateral angular cable rates ($\dot{\vartheta}_C$, $\dot{\varphi}_C$) and optionally the cable angles ($\vartheta_C$, $\vartheta_C$) to the slung load damping controller. In the herein presented control law only the angular cable rates in earth-fixed coordinates have been fed back in an additional path parallel to the SCAS. Based on this information the controller creates automatically additional actuator commands which are overlaid to the actuator commands generated by the SCAS and the pilot's manual control in-

puts. As previous research [5, 18] showed, feedback of the angular cable rates in earth-fixed coordinates is able to realize effective load damping.

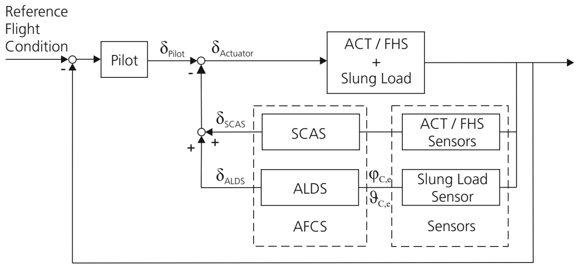


Figure 6: Structure of the control architecture

The control law structure and the optimisation algorithm used herein are adopted from Brenner [16]. Brenner used the idea of loop-shaping to design a slung load stabilisation controller. The idea of loop-shaping is to modify the open-loop frequency responses by controllers to achieve sufficiently high phase and gain margins. The relevant frequency responses are $G_{\delta x \dot{\vartheta}_C}(s)$ describing the longitudinal open-loop behaviour and $G_{\delta y \dot{\varphi}_C}(s)$ describing the lateral open-loop behaviour.

$$(1) \quad G_s(s) = \begin{cases} G_{\delta_x \dot{\vartheta}_c}(s) \\ G_{\delta_y \dot{\varphi}_c}(s) \end{cases}$$

Each axis is controlled separately without cross-coupling. The controller transfer function structure $G_R(s)$ is the same for both axes. Only the control parameter values after optimisation are different. The controllers for both pendulum directions consist of two transfer functions $G_{PM}(s)$and $G_{AM}(s)$. The lead-lag filter element $G_{PM}(s)$ is used to adjust the phase margin and lead-lag filter element $G_{AM}(s)$ to adjust the gain margin.

$$(2) \quad G_R(s) = G_{PM}(s) G_{AM}(s)$$

$$(3) \quad G_{PM}(s) = k_{0dB} \frac{1}{\sqrt{m_{PM}}} \frac{1 + \frac{s}{\omega_{E1}}}{1 + \frac{s}{\omega_{E2}}}$$

$$(4) \quad G_{AM}(s) = \frac{1 + \frac{s}{\omega_{E3}}}{1 + \frac{s}{\omega_{E4}}}$$

$$(5) \quad G_R(s) = k_{0dB} \frac{1}{\sqrt{m_{PM}}} \frac{1 + \frac{s}{\omega_{E1}}}{1 + \frac{s}{\omega_{E2}}} \frac{1 + \frac{s}{\omega_{E3}}}{1 + \frac{s}{\omega_{E4}}}$$

### 2.3.3. Optimisation Algorithm

The controller structure is closely linked to the optimisation algorithm. In the following section a brief summary of the optimisation process is given. Details of the optimisation algorithm are described in Ref. [16]. First of all the gain response is lifted by the proportional gain ($k_{0dB}$) until the gain crossover frequency ($\omega_d$) equals the pendulum frequency ($\omega_P$). Therefore, the quickness of the controller is fitted to the system's natural frequency. The pendulum frequency can be approximated using Eqn. (6). This equation describes the frequency of a mathematical double-pendulum model and can be used as good approximation of the slung load pendulum frequency.

$$(6) \quad \omega_P = \sqrt{\frac{g}{L}(1 + \frac{m_L}{m_H})}$$

The phase response is modified using the lead-lag element of the phase modulation controller ($G_{PM}(s)$) in Eqn. (3). Depending on the actual phase value, the phase response has to be lifted or lowered at the point of the gain crossover frequency to achieve the actual desired phase margin ($\Phi_{PM,cmd}$). The actual desired phase margin is varied in the interval between 60 deg and 90 deg using a step size of 1 deg. The modification of the phase response also influences the amplitude response, thus the amplitude response is corrected using the correction parameter ($m_{PM}$) to maintain the gain crossover frequency.
In the next optimisation stage, the amplitude response is modified using the lead-lag element of the gain modulation controller ($G_{AM}(s)$ in Eqn. (4)) to reach the desired gain margin value ($A_{GM,cmd}$). Therefore, $\omega_{E3}$ is varied in the interval between 0.1 rad/s and 1.0 rad/s with a step size of 0.1 rad/s. Due to the modulation of the amplitude response, the phase response is affected again. This is evaluated automatically in the following calculation of the performance index $J$ to find the optimal controller parameter setting.

$$(7) \quad J = K_V(\omega_{d,perc.} + (\Phi^3_{PM,perc.} + A^3_{GM,perc.})10^{-4})$$

The percental differences between the desired target values and the actual values for the following requirements are part of the performance index calculation:

**Phase Margin** $\Phi_{PM}$: To achieve a stable system and high damping values for the pendulum motion a target value of 90 deg phase margin is used.

**Gain Margin** $A_{GM}$: To achieve a robust system with adequate disturbance rejection a target value of -12 dB gain margin is applied.

**Crossover Frequency** $\omega_d$: The closed-loop quickness shall be in the range of the system's natural frequency. This can be realised by adjusting the crossover frequency $\omega_d$ to the pendulum frequency $\omega_P$.

Additionally in the calculation of the performance index the static amplification is weighted by $K_V$.

$$(8) \quad K_V = (\frac{k_{0dB}}{\sqrt{m_{PM}}})^{\frac{1}{8}}$$

Therefore, low amplification factors which lead to limited system performance and very high gains, which can drive the system to stability limits, are penalised in the evaluation. Due to the chosen intervals for the variation of $\Phi_{PM,cmd}$ and $\omega_{E3}$, 310 potential control parameter settings are calculated in total for each axis. To find the optimal control parameter setting in reference to the requirements, all performance index values of each axis are compared to each other. The control parameter setting with the maximum performance index value is chosen to be the optimal setting.

#### 2.3.4. Additional Filter

The optical-inertial slung load sensor is mounted under the boom of the recue hoist. During operation the boom of the hoist is vibrating because of the transmission of the helicopter's vibrations. This vibration is detected by the slung load sensor. Thus the signals of the measured angular cable rates show higher frequency content. In addition, the sensor delivers the signals with a frequency of 50 Hz. The controller works with the sample frequency of the ACT/FHS's experimental system of 125 Hz and the 50 Hz frequency content can be transmitted as undesired actuator commands. Both the frequency content of the vibrations and the sampling effect have to be removed before using the signal for the feedback to the helicopter actuators. Therefore a second-order Butterworth-Filter is used. This filter influences the response characteristics between the controls and the angular cable rates. Hence, the transfer function of the filter is additionally considered in the control parameter optimisation.

#### 2.3.5. Simulation Results

The main objective of this work was to demonstrate the principal of controlling a slung load suspended from a rescue hoist in flight. Due to limited flight test time in preparation of the tests, a selection of limited slung load parameters had to be made. For that purpose, all performance indices of the optimal control parameter settings were compared for different cable lengths and load masses. Based on the model data, best controller performance could be expected for high load masses and cable lengths of approximately 20 m. Due to the maximum take-off weight of the ACT/FHS the load mass is limited to 100 kg. A load mass of 100 kg and a cable length of 20 m were selected for flight tests and were used for simulations.

Analyses with the control law in preparation of flight tests were completed in two stages. In the first stage, the slung load simulation on a desktop computer was used. In the second stage the nonlinear simulation in the realtime environment of the ACT/FHS ground-based system simulator was utilized. The system simulator provides a hardware/software in the loop simulation with a nonlinear helicopter model [19]. All hardware and software modifications are tested in the system simulator before flight testing. Due to the lack of suitable flight test data the used slung load models could not be validated even after the initial flight tests presented in this paper. Instead several plausibility checks were accomplished including comparison of the pendulum frequencies to analytical calculations as well as the influence of the drag coefficient, flight speed and on the trailing angle of the slung load.

To check the efficiency of the chosen control law in damping the load swing, the load was excited to swing due to control inputs in longitudinal axis. The behaviour of the load with and without activated ALDS was compared. Fig. 7 displays the results from the desktop simulation. In Fig. 7(a) and 7(e) the additional slung load control inputs are shown ($\delta_{ALDS,x}$, $\delta_{ALDS,y}$). In Fig. 7(b) and 7(f) final actuator commands are shown ($\delta_{Act,x}$, $\delta_{Act,y}$), followed by the helicopter's attitude ($\Theta_{H,e}$, $\Phi_{H,e}$, Fig. 7(c), 7(g)) and the pendulum angles in inertial coordinates($\vartheta_{C,e}$, $\varphi_{C,e}$, Fig. 7(d), 7(h)). After an initial control input the helicopter's change in attitude forces the load to swing. Without ALDS the load oscillation is unstable. In the cases where the ALDS is activated the controller calculates additional actuator commands to suppress the load swing. The controller shows good on- and off-axis damping of the load swing (Fig. 7(h)). Fig. 8 shows the results from the nonlinear simulation. To excite the slung load swing motion, automatically generated actuator commands were used. These are not exactly the same inputs as used in Fig. 7 because of some differences in the fidelity of the used helicopter models. Therefore, the plots cannot be compared directly. Fig. 8(h) shows that the oscillation of the slung load can be also damped by the ALDS in the nonlinear simulation.

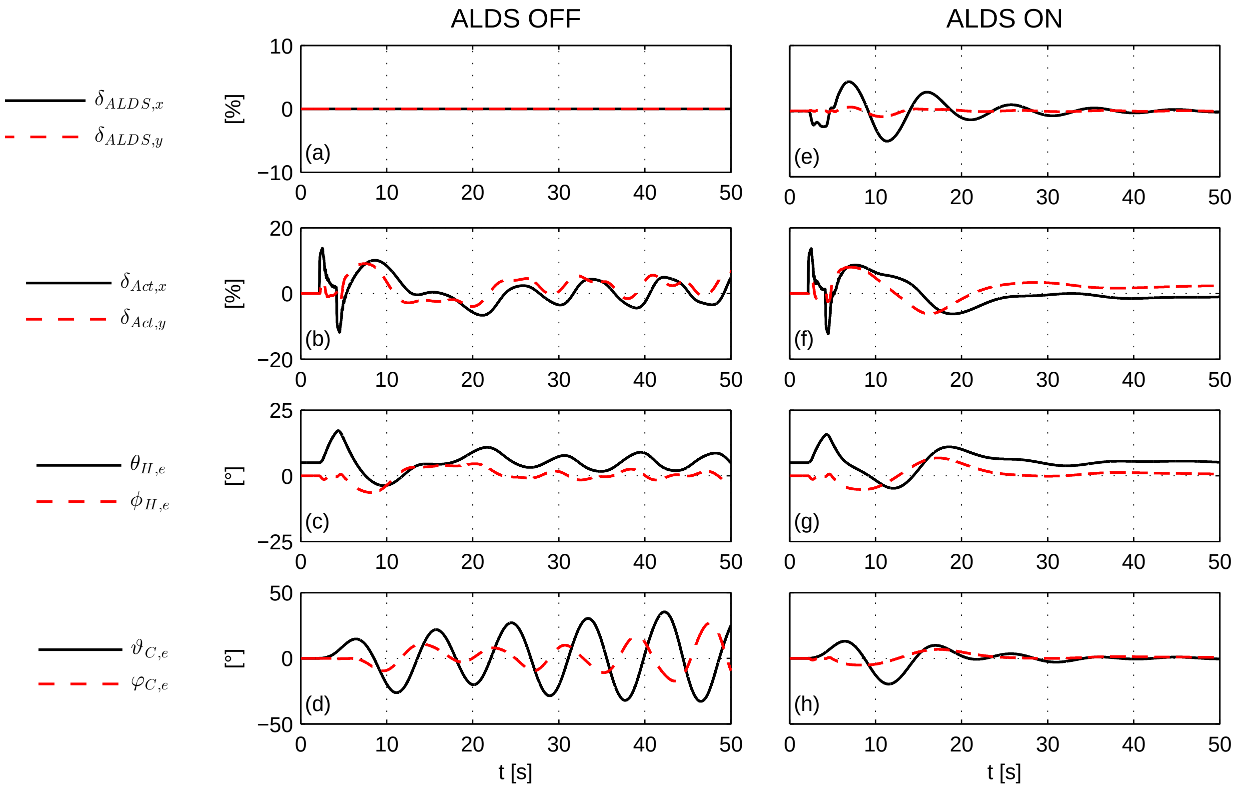


Figure 7: Desktop simulation - excitation of the load swing in longitudinal direction

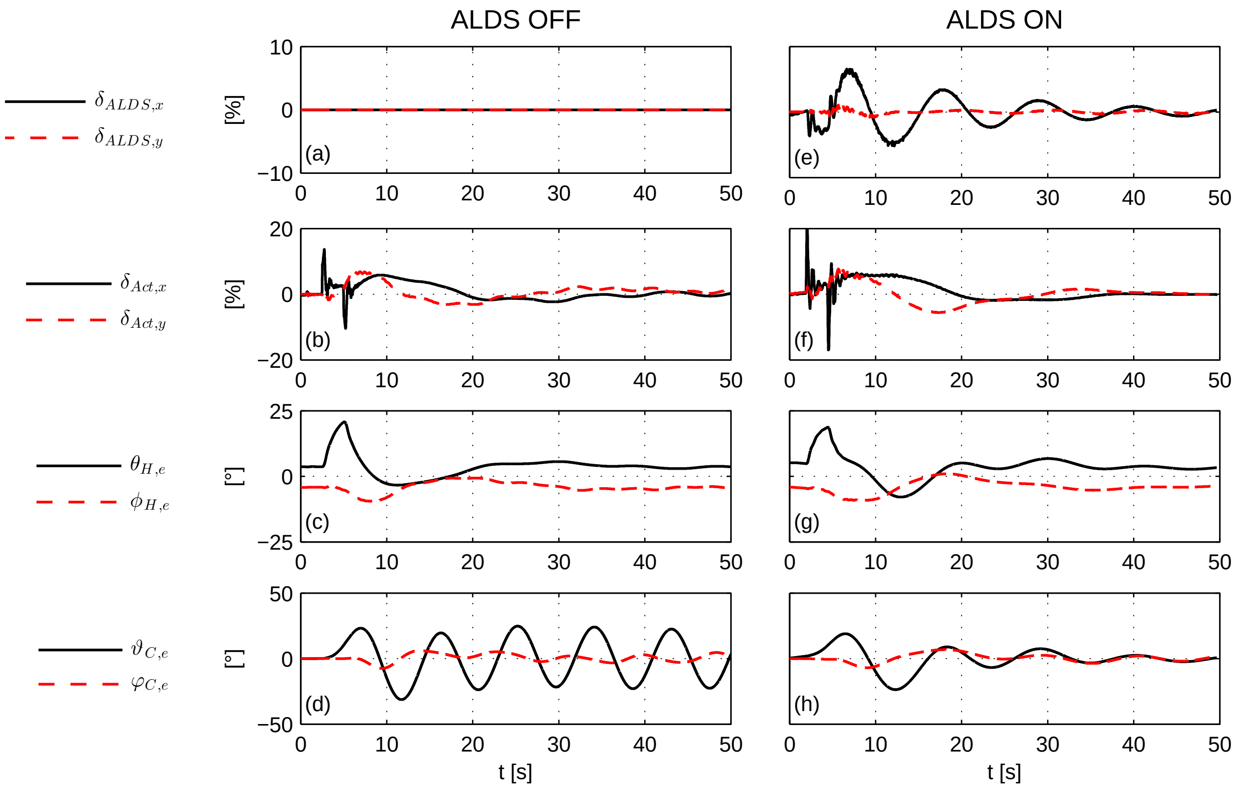


Figure 8: Nonlinear simulation - excitation of the load swing in longitudinal direction

## 3. FLIGHT TESTS

### 3.1. Flight test preparations

Considerable effort was required before the sensor system was approved for flight. The optical-inertial sensor and optical marker were tested against vibration and high shock loads. Due to the sensor mounting on the hoist boom and the additional weight of both the sensor and marker, a resonance test of the system on the ground was necessary. Analysed results indicated potential resonance problems requiring some modifications to the adapter and sensor housing.
To cope with the maximum cable length of 50 m, the optical marker uses a large number of LED lights associated with a high emission power. This resulted in a classification of the marker as a laser which required protection measures with the activated marker.
A dummy of 100 kg with high density and low drag area was selected as test load. Since it was the first time that DLR's ACT/FHS was operated with an external load and rescue hoist, the flight and ground crew were enabled to get familiar with rescue hoist operation during the first flights (e.g. load pick-up and set-down).
The orientation of the optical sensor on the hoist boom was initially set in such a way that the landing gear was not in the camera's FOV. The suspension of the load causes the hoist boom to bend, causing part of the landing gear to appear in the FOV, leading to the sun reflections in the left corner of Fig. 9. After adjusting of the sensor mounting on the hoist boom, no further reflections of the landing gear were recorded.


Figure 9: Image of the camera showing the optical marker and sunlight reflections from the landing gear before correct camera adjustment

As mentioned before, to avoid unfavourable cable contact with the landing gear, the load motion was excited mainly in longitudinal direction by a longitudinal reposition manoeuvre of the helicopter. While observing the display with the load motion, the pilot noted that input control in the pedal was useful in controlling the load motion.

### 3.2. Flight testing of the sensor system

Comprehensive flight testing of the sensor system was conducted in order to check its functionalities optical marker detection, estimation of cable length as well as estimation of cable angle and cable angle rates. The detection of an optical marker with a diameter of maximum 0.2 m in a distance between 3 m and 50 m was one of the challenges. The proper sensor setting for the distinction between the marker blob and possible interference blobs caused by sunlight reflections was one of the main task during the sensor testing.
The reliable estimation of the cable length and the cable angles as well as cable angle rates had to be proved as a prerequisite for using the signals for the slung load damping control. Main flight test results of the sensor system are presented and discussed below.

#### 3.2.1. Comparison between iVRU and helicopter reference system solutions

The recorded flight test data allows a comparison between the measurements of the MEMS based iVRU-BB from iMAR Navigation GmbH and the helicopter internal reference (ring laser gyro based H764 from Honeywell International Inc.). The differences in acceleration and angular rate measurements as well as position and velocity solutions are low. The comparison of the angular rate and velocity signals are displayed in Fig. 10(b)-(d) and Fig. 10(a) respectively. The system mounted under the boom of the rescue hoist experiences slightly different dynamics (e.g. larger vibrations) than the helicopter's reference system.

#### 3.2.2. Marker detection

The sophisticated image processing assures a reliable identification of the optical marker in a real world environment. This was proven for distances up to 50 m during flight tests. The light signal of the optical marker which is positioned in a distance of 3 m is shown in Fig. 11.

The reliable detection of the optical marker which is hoisted from a level of 50 m below the optical-inertial sensor to a level of 30 m below the optical-inertial sensor is shown in Fig. 12. The helicopter's attitude is shown in Fig. 12(a). The helicopter excites the longitudinal load pendulum motions by a longitudinal reposition manoeuvre after 135 seconds from the start of recording. The longitudinal marker position in the camera image and the longitudinal cable angle are shown in Fig. 12(b) and the lateral marker position in the camera image and the lateral cable angle are shown in Fig. 12(c), respectively. Fig. 12(d) shows the longitudinal and lateral cable angle rates.
The computed correlation between the detected marker signal in the camera image and the expected marker signal in

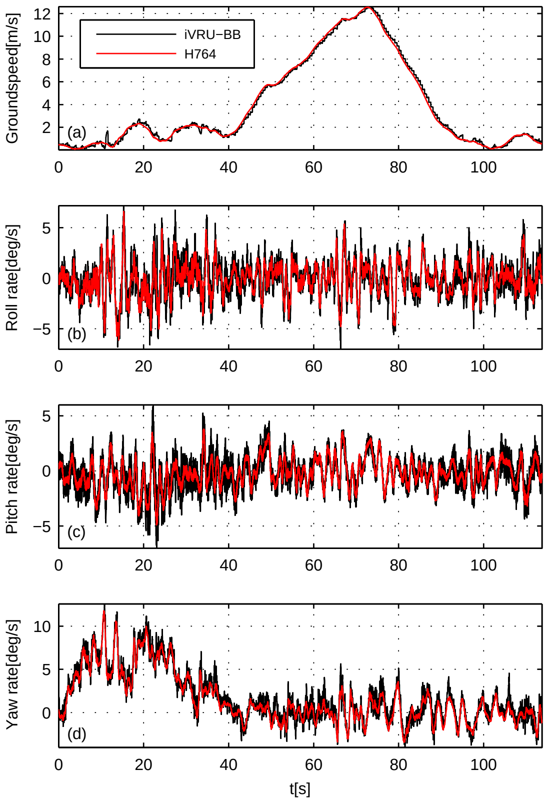


Figure 10: Helicopter angular rates and groundspeed

the image is shown in Fig. 12(e). After 33 seconds of the record's begin, the marker is outside the camera's FOV for several seconds indicated by a minimum correlation value of zero. The cable length estimation for this and all following figures is activated. The estimated cable length is shown in Fig. 12(f).

#### 3.2.3. Cable angles and cable angle rates estimation

An assessment of the accuracy of cable angle and cable angular rate estimation is obtained by consideration of the position of the optical marker in the camera image provided by image processing and the absolute cable angles provided by the Kalman filter. The evaluation of the flight test data shows a clear correlation between the marker position and the absolute cable angles in terms of frequency and phase (see Fig. 13(b) and Fig. 13(c)).

In case that the optical marker is outside the camera's FOV, there is no marker signal to detect in the camera image. As a result the correlation between the marker signal in the camera image and the expected marker signal is zero. Figure Fig. 14 shows permanent estimation of cable angles and cable angular rates even if the optical marker is temporarily outside the camera's FOV. There are no steps in cable angles and cable angle rates when the optical marker re-enters the camera's FOV.

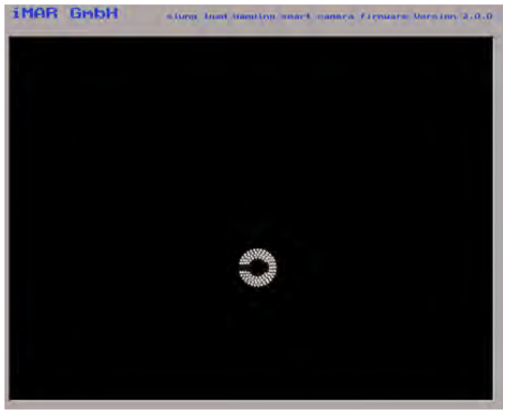


Figure 11: Image of the camera showing the light signal of the optical marker positioned in a distance of 3 m (raw camera image)

#### 3.2.4. Cable length estimation

In the framework of the project HALAS, it was not possible to realize a data connection between the experimental system of the ACT/FHS and the rescue hoist. Therefore, the cable length could not be obtained from the rescue hoist. For this reason, a fast and precise estimation of the cable length is provided by the Kalman filter running on the control unit of the optical-inertial sensor. For example, a cable length of 20 m is determined correctly in less than 15 seconds after activation of the estimation process (see Fig. 15(f)).
From analysis of the flight data it can be concluded that the cable length is estimated properly up to the maximum tested length of 50 m. The estimation process will be used if no external cable length signal is available. It is planned to connect the rescue hoist with the experimental system in the future so that the actual cable length can be used directly.

### 3.3. Flight testing of the slung load damping control

The final test of the herein presented control law was conducted in real flight testing using the ACT/FHS equipped with a rescue hoist system. Flight testing of the control system was conducted in several stages. In the first stage, the used SCAS parameter settings were tested with the attached rescue hoist and slung load. Afterwards the filter settings of the used Butterworth-Filter and a function to fade-in the controller were tested open-loop. To show the feasibility of the control law concept, closed-loop tests followed. During the flight tests, the test pilot commented that he feels controlling against the active ALDS. The left column in Fig. 16 shows such a situation. In this case, the helicopter

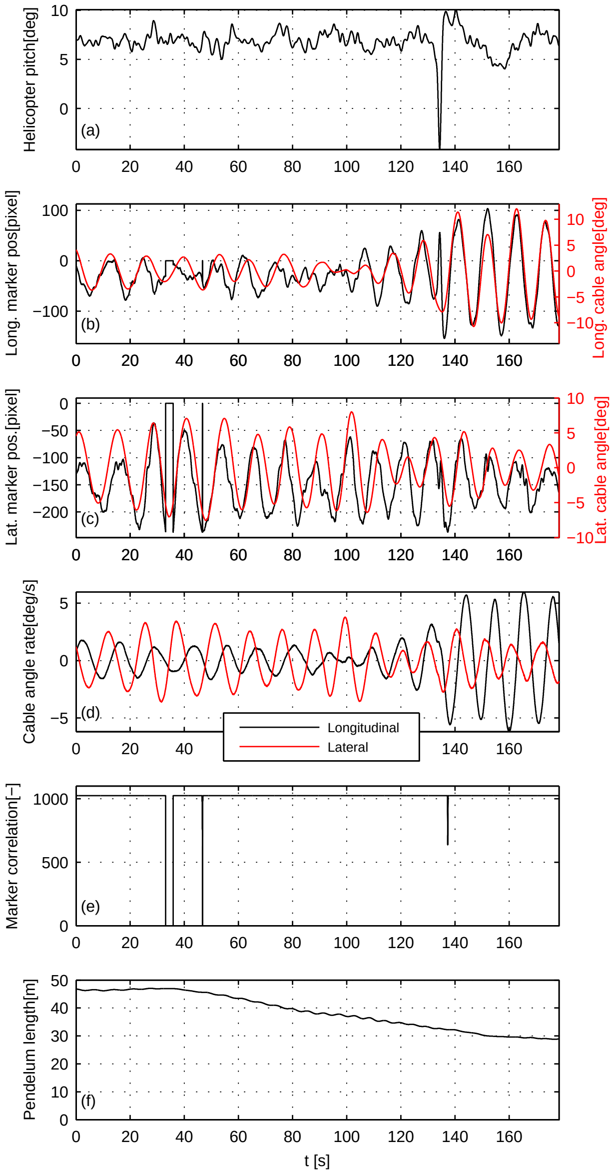


Figure 12: Reliable marker detection in a distance between 50 m and 30 m

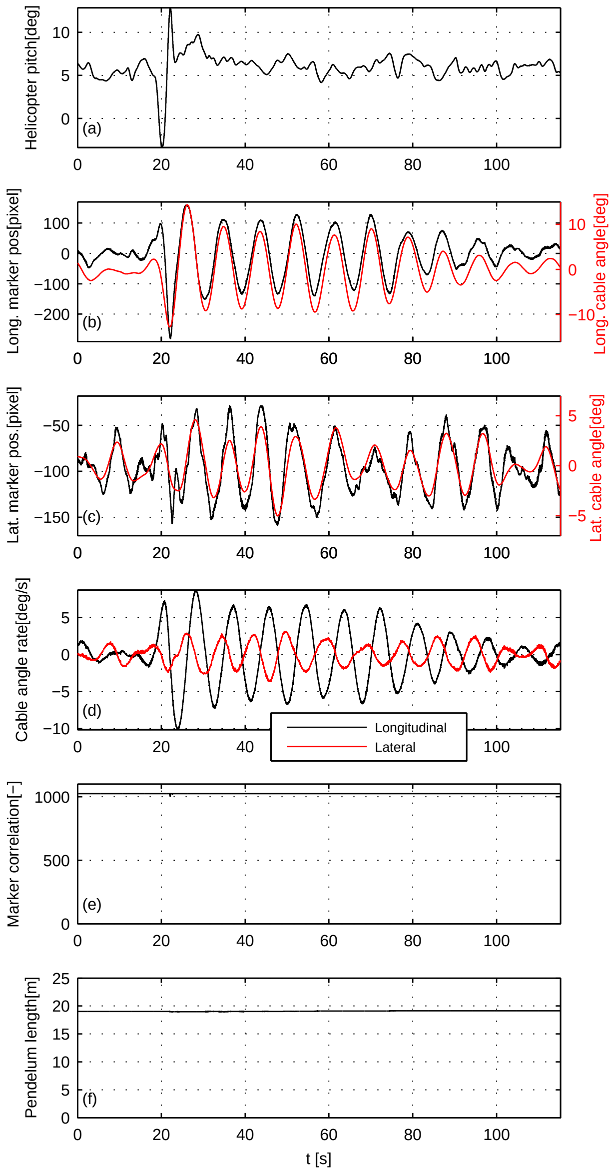


Figure 13: Correlation between marker position and absolute cable angles

was hovering with an initially vertical hanging load swinging around 3 deg in longitudinal axis. After approximately 10 s the ALDS was switched on. Due to the small load swing, the controller started to generate additional actuator commands intended to stabilize the load by the helicopter's change in attitude and position.

Fig. 16(c) shows how the pilot is controlling ($\delta_{Pilot,x}$) versus the commands generated by the ALDS ($\delta_{ALDS,x}$). This excites the load swing. After switching off the ALDS a lightly damped load pendulum motion can be noticed. Compared to the simulation results in Fig. 7(d) and 8(d), the load motion exhibits a higher damping indicating a discrepancy in the simulation model. This discrepancy will be treated in further research work (e.g. by adopting the aerodynamic drag of the load simulation model).

Helicopter pilots are accustomed to hold the helicopter's position in hover. For that purpose, they are using visual reference points in the surrounding area as well as the visual cues of the primary flight display and the motion cues. With the activated ALDS, the pilot is not able to distinguish between disturbances in the helicopters attitude and position due to small wind gusts and intended changes in attitude and position to damp the load swing. The activated ALDS degrades the ability of the pilot to hold the helicopter position. Furthermore due to the feedback of the load pendulum motion, the helicopter reacts to pilot stick inputs, commanding additional responses to stabilise the load. For this reason, the helicopter responses to stick inputs become unpredictable for the pilot.

This can result in degraded HQ as previous research by AFDD (US Army Aeroflightdynamics Directorate) has shown [5, 18]. The conflict between good load damping char-

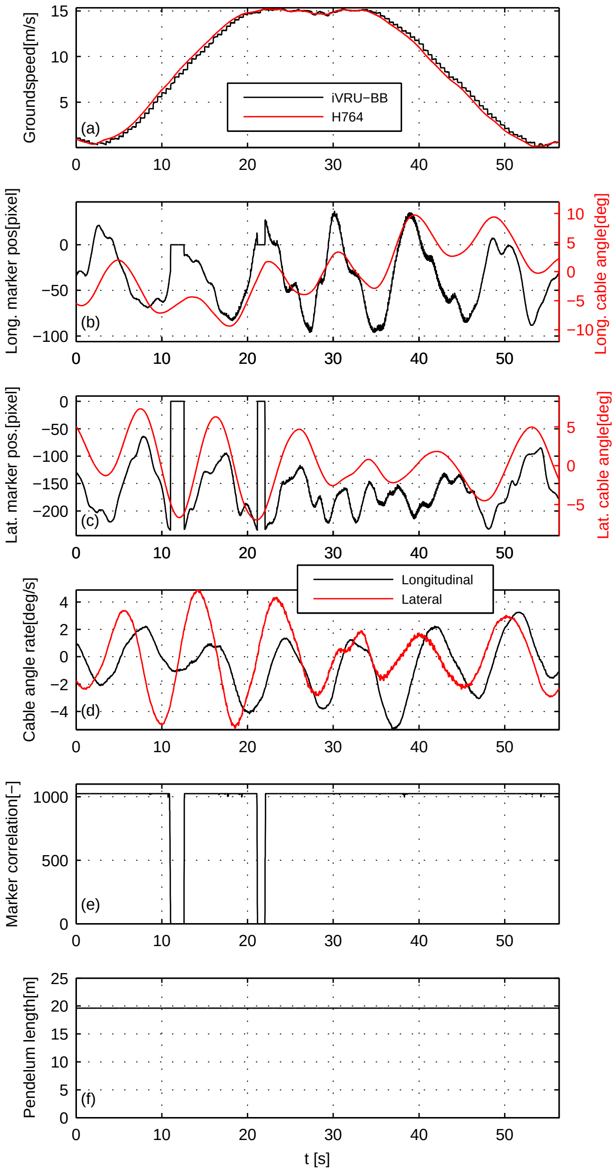


Figure 14: Correlation between marker position and absolute cable angles (marker temporarily out of FOV)

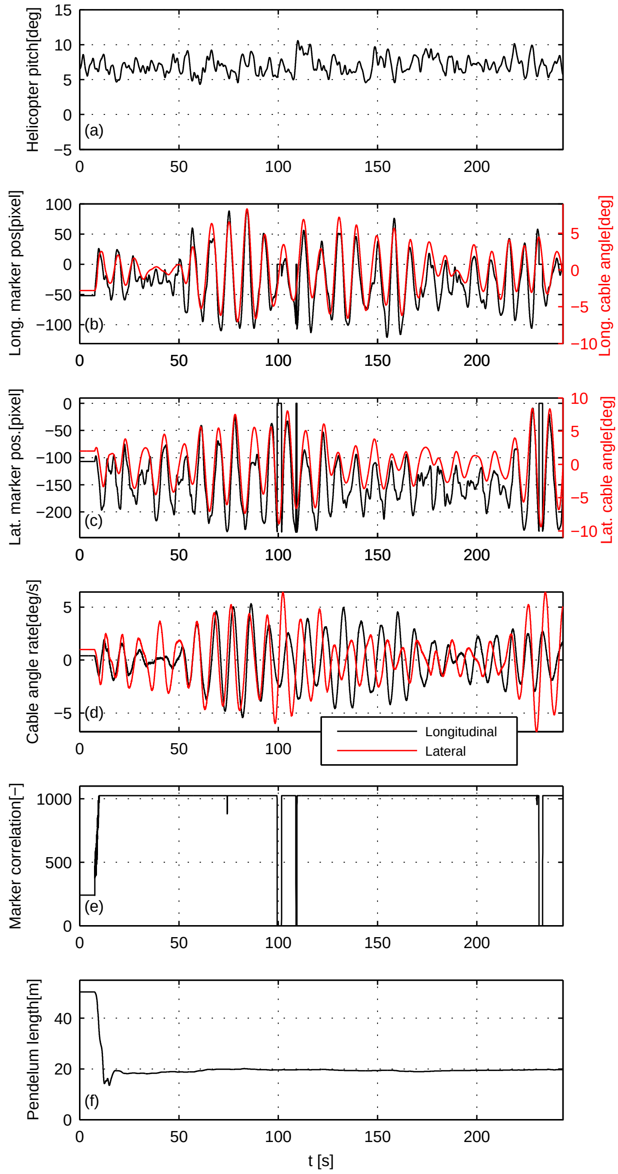


Figure 15: Cable length estimation of a fixed cable length of 20 m

acteristics and HQ aspects has been previously identified and examined by Ivler et al. In the currently used parameter optimisation method presented herein HQ aspects are not included as design specifications. For future work, an improved parameter optimisation method including HQ criteria is planned to be applied.

In the right column of Fig. 16 the results of a trial are shown where the pilot excited the load motion and then exited the control loop. The ALDS successfully damped the on-axis load swing in longitudinal direction. In off-axis the load damping was not effective (not shown in the figure).

In Fig. 17 a comparison between two trials with comparable initial cable angles after load swing excitation at approximately the same time is shown. In this comparison damping of load swing in the longitudinal axis by the ALDS can be recognized (see Fig. 17(h)). To identify the reason for the reduced effectiveness of the controller in lateral axis will be part of future work.

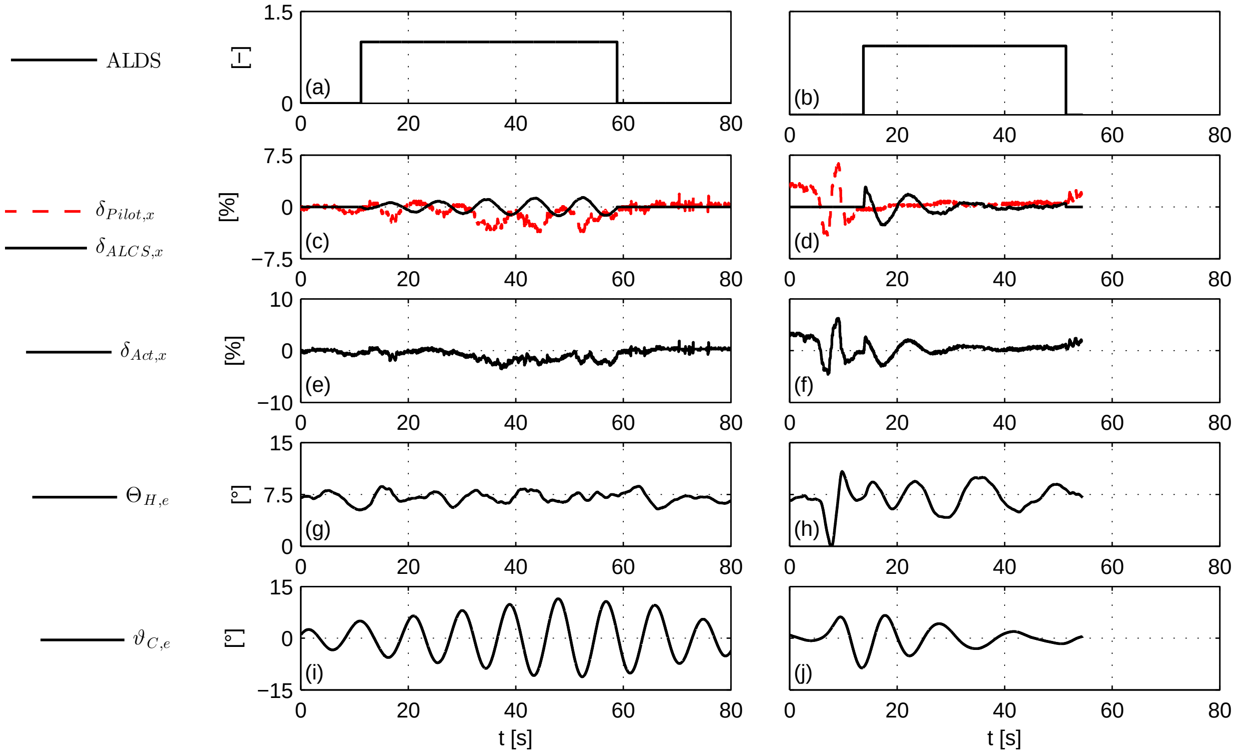


Figure 16: Flight test - interaction between pilot and controller

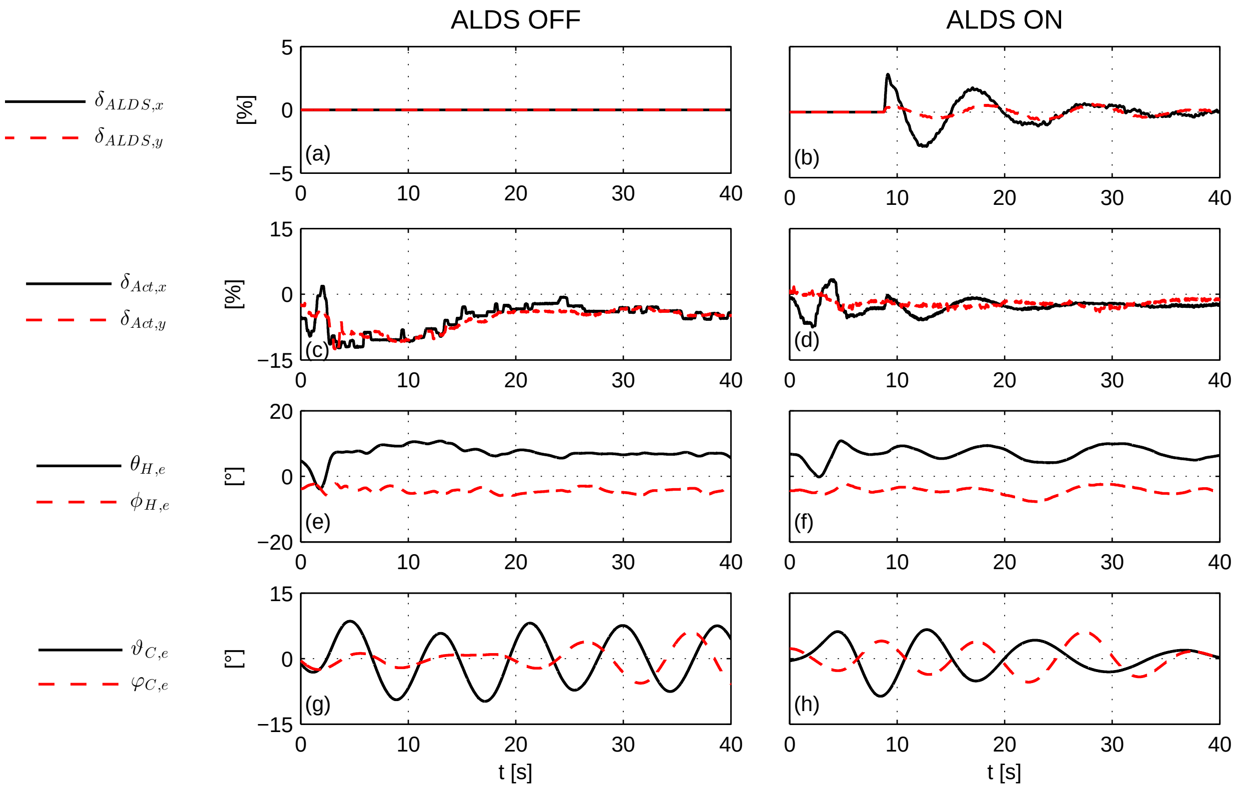


Figure 17: Flight test - excitation of the load swing in longitudinal direction

## 4. Conclusion

The results of initial flight tests of an automatic slung load control system for DLR's research helicopter ACT/FHS were presented. The main results of this work are listed in the following.

1. A slung load control system for a helicopter with a rescue hoist was developed and flight tested.
2. For load motion detection, an optical sensor system was developed. The optical-inertial sensor system has reliably detected the position of the optical marker in distances up to 50 m. The inertial and relative load motion information and the cable length information provided by the optical-inertial sensor system were sufficiently precise for control purposes based on the results of the initial flight tests.
3. An automatic control system for slung load damping was designed by augmenting the helicopter's SCAS. The controller parameters were determined using a frequency loop-shaping algorithm.
4. The automatic slung load control function could effectively damp the load pendulum motion in longitudinal direction for a fixed cable length.
5. Under piloted control, a conflict between controlling the helicopter by manual and automatic load control was evident.

## 5. Outlook

The experimental slung load control system is now ready for operation and the following research work will be focused on the design of load control systems. Planned modifications of the system and control design are as follows:

- A data link from the rescue hoist to the ACT/FHS will be installed so that the actual cable length will be available for the optical-inertial sensor and control system.
- The design of the slung load damping system will be adapted to consider design specifications related to piloted operations. The load control system will be extended by an automatic load positioning function and tested in flight.
- Synchronisation of image acquisition and light emitting will be demonstrated in future flight tests. It is planned to integrate a second camera in the optical-inertial sensor to provide a top-down view of the load and the ground below to the pilot. Furthermore, a second optical marker will be used to mark a desired location (e.g., a platform on a vessel) for load pick-up and set-down.

## 6. Acknowledgement

The project HALAS was part of the German Federal Aeronautical Research Program (LuFo IV-3). DLR and iMAR would like to acknowledge the BMWi for funding the project HALAS. The authors wish to thank all the persons who were involved in this project and supported the flight tests, namely Robin Lantzsch with his team and the DLR facility Flight Experiments at Braunschweig. We are grateful for the invaluable support of the department of Flight Test Instrumentation, especially Klaus Alvermann, and the whole team of Torsten Gerlach. Thanks also to Herbert Graser who contributed as test pilot.

## References

[1] Manwaring, J. C. ; Conway, G. A. ; Garrett, L. C.: *Epidemiology and Prevention of Helicopter External Load Accidents*. Journal of Safety Research, Vol. 29, No. 2, pp.107-121(15), 1998

[2] Lusardi, J. A. ; Blanken, C. L. ; Braddom, S. R.: *UH-60 External Load Handling Qualities Evaluation*. Proceedings of the 35th European Rotorcraft Forum, Hamburg, Germany, 2009

[3] Lusardi, J. A. ; Blanken, C. L. ; Braddom, S. R. ; Cicolani, L. S. ; Tobias, E. L.: *Development of External Load Handling Qualities Criteria for Rotorcraft*. Proceedings of the 66th Annual Forum of the AHS International, Phoenix, AZ, 2010

[4] US Army Aviation and Missile Command: *Handling Quality Requirements for Military Rotorcraft*. Aeronautical Design Standard, Technical Report ADS-33E-PRF, U.S. Army Aviation and Missile Command (USAAMCOM), Redstone Arsenal, Alabama, 2000

[5] Ivler, C. M. ; Powell, J. D. ; Tischler, M. B. ; Fletcher, J. W. ; Ott, C.: *Design and Flight Test of a Cable Angle/Rate Feedback Flight Control System for the RASCAL JUH-60 Helicopter*. Proceedings of the 68th Annual Forum of the AHS International, Fort-Worth, TX, 2012

[6] Nonnenmacher, D. ; Kim, H. ; Götz, J. ; Weber, P. ; Hinüber, E. von ; Knedlik, S.: *System Architecture of HALAS - A Helicopter Slung Load Stabilisation and Positioning System*. CEAS Aeronautical Journal, 2013

[7] Mansur, M. H. ; Bielefield, M. D. ; Cheung, K. K.: *Full Flight Envelope Inner-Loop Control Law Development for the Unmanned K-MAX*. Proceedings of the 67th Annual Forum of the AHS International,Virginia Beach, Virginia, 2011

[8] McGonagle, J. G.: *The Design, Test, and Development Challenges of Converting the K-MAX Helicopter*

*to a Heavy Lift Rotary Wing UAV*. Proceedings of the 57th Annual Forum of the AHS International, Washington, DC, 2001

[9] BISGAARD, M. ; COUR-HARBO, A. la ; JOHNSON, E. N. ; BENDTSEN, J. D.: *Vision Aided State Estimator for Helicopter Slung Load System*. Proceedings of the 17th IFAC Symposium on Automatic Control in Aerospace, Toulouse, France, 2007

[10] KANG, K. ; OTTANDER, J. ; PRASAD, J. V. R. ; JOHNSON, E.: *Active Control of a UAV Helicopter with a Slung Load for Precision Airborne Cargo Delivery*. Proceedings of the 66th Annual Forum of the AHS International, Phoenix, AZ, 2010

[11] OTTANDER, J. A. ; JOHNSON, E. N.: *Precision Slung Cargo Delivery onto a Moving Platform*. Proceedings of the AIAA Modeling and Simulation Technologies Conference, Toronto, Ontario, Canada, 2010

[12] BERNARD, M. ; KONDAK, K. ; HOMMEL, G.: *Load Transportation System based on Autonomous Small Size Helicopters*. The Aeronautical Journal, Vol. 114, No. 1153, pp. 191-198(8), 2010

[13] HAMERS, M. ; BOUWER, G.: *Helicopter Slung Load Stabilization Using a Flight Director*. Proceedings of the 61st Annual Forum of the AHS International, Grapevine, Texas, 2005

[14] HAMERS, M. ; HINÜBER, E. von ; RICHTER, A.: *CH53G Experiences with a Flight Director for Slung Load Handling*. Proceedings of the 64th Annual Forum of the AHS International, Montreal, Canada, 2008

[15] KALETKA, J. ; KURSCHEID, H. ; BUTTER, U.: *FHS, the New Research Helicopter: Ready for Service*. Proceedings of the 29th European Rotorcraft Forum, Friedrichshafen, Germany, 2003

[16] BRENNER, H.: *Helicopter Sling Load Pendulum Damping*. Proceedings of the 35th European Rotorcraft Forum, Hamburg, Germany, 2009

[17] GREISER, S. ; LANTZSCH, R.: *Equivalent Modelling and Suppression of Air Resonance for the ACT/FHS*. Proceedings of the 39th European Rotorcraft Forum, Moscow, Russia, 2013

[18] IVLER, C. M. ; TISCHLER, M. B. ; POWELL, J. D.: *Cable Angle Feedback Control Systems to Improve Handling Qualities for Helicopters with Slung Loads*. Proceedings of the AIAA Guidance, Navigation and Control Conference, Portland, Oregon, 2011

[19] HAMERS, M. ; GRÜNHAGEN, W. von: *Nonlinear Helicopter Model Validation Applied to Realtime Simulations*. Proceedings of the 53rd Annual Forum of the AHS International, Virginia Beach, Virginia, 1997